




# Adhesion in thermomechanically processed seaweed-lignocellulosic composite materials

Paul Grandgeorge, Ian R. Campbell, Hannah Nguyen, Rebekah Brain, Mallory Parker, Scott Edmundson, Deborah Rose, Khadijah Homolke, Chinmayee Subban, and Eleftheria Roumeli\* 

Received: 21 February 2024 / Accepted: 24 April 2024 / Published online: 19 June 2024

## Impact statement

This research introduces a sustainable alternative to petroleum-derived adhesives used in wood-based panels, addressing a pressing environmental concern in our infrastructure and construction materials. Here, we discuss the use of *Ulva*, a green seaweed species, as a renewable and biodegradable solution for such adhesives. We demonstrate its efficacy as a bonding agent in hot-pressed wood panels, offering enhanced strength and durability. Moreover, the use of *Ulva* contributes to mitigating the environmental footprint associated with traditional materials, aligning with global efforts toward sustainability and circular economy principles. Through comprehensive spectroscopic analyses and mechanical testing, we provide insights into the underlying mechanisms of *Ulva*-based adhesion. Furthermore, we report the water resistance and improved flame retardancy of *Ulva*-bonded wood, which are essential for applications in infrastructure and construction. Finally, we discuss environmental and social advantages of *Ulva*-based composites.

The increasing concerns associated with petroleum-derived polymers motivate the development of sustainable, renewably sourced alternatives. In ubiquitous applications such as structural materials for infrastructure, the built environment as well as packaging, where natural materials such as wood are used, we rely on nonrenewable and nondegradable polymers to serve as adhesives. In wood panels, such as medium density fiberboards (MDFs), formaldehyde-based resins are predominantly used to bond wood fibers and to provide strength to the materials. To further mitigate the environmental impact of construction materials, more sustainable adhesives need to be investigated. In this article, we introduce *Ulva* seaweed as an adhesive to enable cohesion and strength in hot-pressed wood panels. Upon hot-pressing, powdered *Ulva* flows in between the wood particles, generating a matrix, which provides strong binding. We show that the flexural strength of *Ulva*-bonded wood biocomposites increases with increasing *Ulva* concentrations. At an *Ulva* concentration of 40 wt%, our composites reach an average elastic modulus of 6.1 GPa, and flexural strength of 38.2 MPa (compared to 4.7 GPa and 22.6 MPa, respectively, for pure wood compressed at the same pressing conditions). To highlight the bonding mechanisms, we performed infrared and x-ray photoelectron spectroscopy and identified indications of fatty acid mobility during hot-pressing. In addition, we demonstrate that the presence of *Ulva* improves other properties of the composites such as water resistance and flame retardancy. *Ulva* is also shown to behave as an excellent adhesive agent between two prepressed beams. Finally, we perform an in-depth analysis of the environmental impact of wood-*Ulva* biocomposites.

## Introduction

Wood-based particleboards and fiberboards are used extensively for packaging solutions and in the construction industry. In 2021, the combined production of particle- and

fiberboards reached 210 million m<sup>3</sup>.<sup>1</sup> Unlike straight wood planks cut out directly from timber, reconstituted particle- and fiberboards can be molded into custom shapes and thicknesses. In industrial production,

Paul Grandgeorge, Department of Materials Science and Engineering, University of Washington, Seattle, USA

Ian R. Campbell, Department of Materials Science and Engineering, University of Washington, Seattle, USA

Hannah Nguyen, Department of Materials Science and Engineering, University of Washington, Seattle, USA

Rebekah Brain, Department of Materials Science and Engineering, University of Washington, Seattle, USA

Mallory Parker, Department of Materials Science and Engineering, University of Washington, Seattle, USA

Scott Edmundson, Pacific Northwest National Laboratory, Seattle, USA

Deborah Rose, Pacific Northwest National Laboratory, Seattle, USA

Khadijah Homolke, Pacific Northwest National Laboratory, Seattle, USA

Chinmayee Subban, Pacific Northwest National Laboratory, Seattle, USA

Eleftheria Roumeli, Department of Materials Science and Engineering, University of Washington, Seattle, USA; eroumeli@uw.edu

\*Corresponding author

doi:10.1557/s43577-024-00734-5



the necessary adhesion between wood particles/fibers is most often achieved using formaldehyde-based synthetic adhesives such as, for example, urea formaldehyde or phenol-formaldehyde to ensure overall cohesion and strength.<sup>1</sup> Although such adhesives offer excellent bonding, performance reliability, and workability,<sup>1</sup> they are generally accepted to be the most costly raw material of particleboards.<sup>2</sup> Moreover, these petroleum-derived adhesives significantly limit the recyclability and compostability of wood-based boards. Finally, regular formaldehyde emissions (FEs) pose another major issue regarding health, as the emitted compounds are toxic for humans.<sup>3</sup> To mitigate toxicity of the adhesives, a common strategy consists in incorporating formaldehyde scavengers in the adhesives: a chemical that binds to free formaldehyde, thereby reducing emissions.<sup>4,5</sup> Still, the environmental limitations and health issues raised by synthetic adhesives call for research in the domain of synthetic free wood particleboards. Emerging solutions consist in leveraging the self-binding of wood particles under heat and pressure,<sup>6,7</sup> or the usage of bio-based adhesives such as lignin-derived phenolics,<sup>8</sup> which will fully leverage the benefits of wood-based boards.

The self-binding of wood powders under the effect of heat, pressure, and moisture was demonstrated in the 1930s by Mason.<sup>6</sup> This phenomenon provided an attractive avenue toward manufacturing of binderless particleboards (i.e., without resorting to synthetic adhesives). The self-binding of hot-pressed wood particles can be explained by the pressure-induced flow of lignin, which is softened by temperature and moisture,<sup>9</sup> ultimately promoting binding. In addition, the hydrolysis of hemicelluloses generates low-molecular-weight carbohydrates, which could act as self-binding agents.<sup>10,11</sup> The beneficial effect of the native presence of lignin on hot-pressed sheets was highlighted by Joelsson et al.<sup>8</sup> where the authors fabricated unbleached kraft fiber sheets using hot-pressing. Using this self-binding, several types of binderless boards have been fabricated from different lignocellulosic biomass, ranging from powdered kenaf core under varying pressing conditions by Okuda and Sato,<sup>12</sup> to steam exploded oil palm.<sup>13</sup> The morphological and mechanical properties of boards can further be drastically improved using fine-tuned preprocessing steps on the wood fibers. For example, Yang et al.<sup>14</sup> fabricated extremely strong holocellulose films, reaching elastic moduli of 21 GPa and tensile strengths of 320 MPa. Their approach consisted in delignifying and defibrillating wood fibers while conserving the native hemicellulose coating cellulose nanofibers. Resorting to less intense preprocessing, another study focused on the morphological and mechanical properties of wood panels fabricated from lignocellulosic microfibrils and wood fibers of wood chips treated by kraft pulping.<sup>7</sup> Despite the absence of synthetic adhesives, their microfibrillated lignocellulose boards reached attractive mechanical properties, with elasticity moduli and strengths reaching 20 GPa and 260 MPa, respectively.

Rather than creating binderless wood panels, synthetic adhesives, such as phenol-formaldehyde (PF), can be replaced

with bio-based adhesives.<sup>1</sup> For example, lignin and tannin, natural polyphenols, have been used to replace varying fractions of synthetic phenol in PF resins.<sup>1</sup> The use of these natural polyphenols not only decreases the consumption of petrochemicals, however, depending on the molecular structure and preprocessing, can form wood adhesives with better mechanical performance<sup>15</sup> or flame resistance<sup>16</sup> than synthetic alternatives. Lignin and tannin have also been combined with additional hardeners,<sup>17</sup> cross-linking agents,<sup>15</sup> and biopolymers<sup>18</sup> to produce adhesives both, including and excluding formaldehyde. Alternatively, proteins extracted from plants (e.g., soy) or from animals (e.g., derived from blood or casein) have been used as bio-based adhesives up to the 1960s, when they started being supplanted by petroleum-based synthetic resins.<sup>14</sup> Natural rubber latex also offers pathways to enable bonding on wood-based particleboards.<sup>19</sup>

Both the binderless (self-binding) or the bio-based adhesive approaches require some level of preprocessing, whether it be to refine the wood particles mechanically and chemically (e.g., micro- or nanofibrillation), or the extraction of specific components to isolate useful bio-based adhesives. These approaches provide convincing results, but such preprocessing steps are energy-intensive and wasteful as only a small fraction of the biological source material is used. Recently, a novel strategy to take advantage of whole biological materials (biomatter) has been proposed in the context of bioplastics (i.e., requiring no preliminary extraction step).<sup>20–23</sup> For example, Iyer et al.<sup>22</sup> showed that using whole algae organisms, with no extraction step and thus no generated waste, hot-pressing induces algae to flow and take the target shape imposed by a mold, finally providing a dense cohesive bioplastic matrix. The spontaneous self-bonding upon hot-pressing, forming stiff and strong plastics, was attributed to the presence of proteins that create a cohesive matrix.<sup>24</sup> Using this flowing and self-bonding behavior of algae powders under heat and pressure could provide an appealing pathway to bio-based adhesives for wood panels with minimal preprocessing and extraction steps.

*Ulva* is a genus of green macroalgae that is commonly found in the rocky intertidal zone worldwide. It can be harvested from the ocean or cultivated in tanks for a variety of purposes, including for human or animal feed, pharmaceuticals, biofuels, fertilizers, and bioremediation.<sup>25–28</sup> More recently, seaweeds like *Ulva* have been considered for materials applications<sup>29–31</sup> and in the context of marine carbon dioxide removal.<sup>32,33</sup>

Here, we take advantage of the self-binding property of algae upon hot-pressing to introduce *Ulva* seaweed as an alternative adhesive to existing synthetic or bio-based adhesives for wood particleboards. Importantly, our boards are composed only of raw wood flour (local woodshop waste) and dried powdered *Ulva* seaweed. We resort to no additives or additional mechanical or chemical preprocessing steps other than grinding down powders. In **Figure 1**, we detail the processing steps followed to fabricate *Ulva*-bonded wood biocomposites using heat and pressure. We

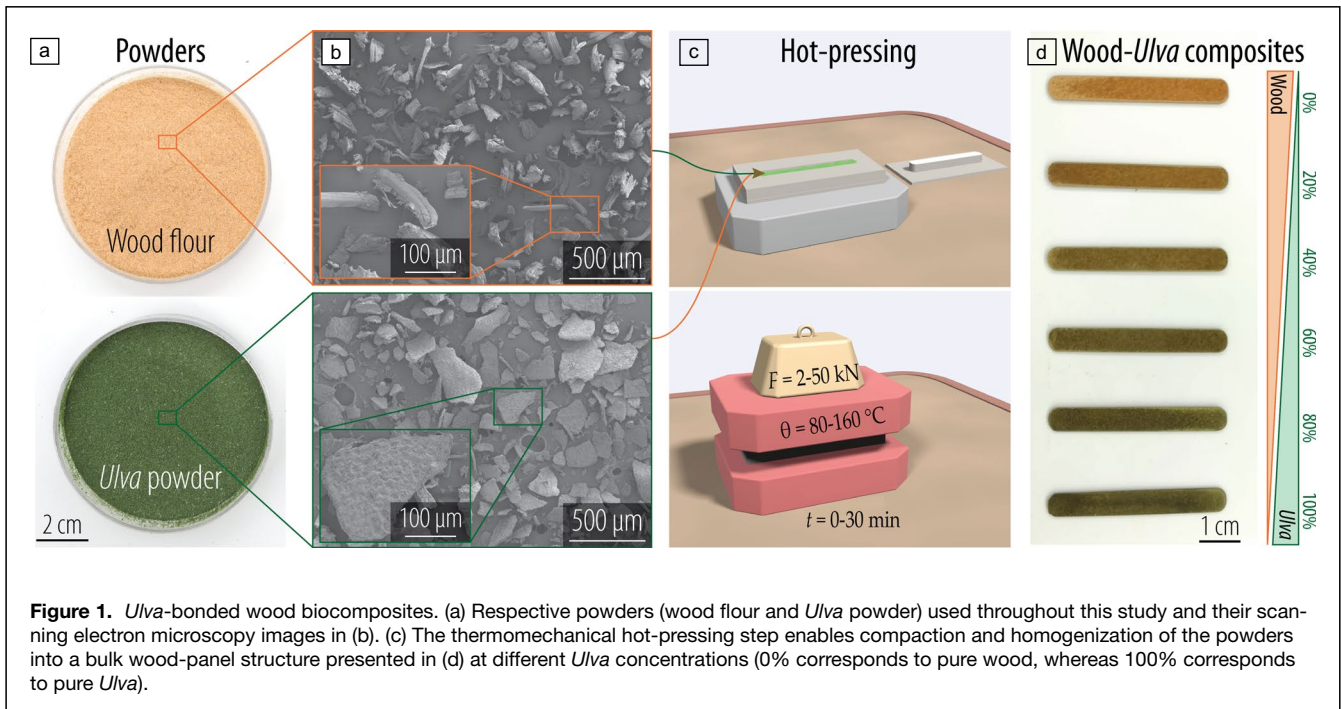


**Figure 1.** *Ulva*-bonded wood biocomposites. (a) Respective powders (wood flour and *Ulva* powder) used throughout this study and their scanning electron microscopy images in (b). (c) The thermomechanical hot-pressing step enables compaction and homogenization of the powders into a bulk wood-panel structure presented in (d) at different *Ulva* concentrations (0% corresponds to pure wood, whereas 100% corresponds to pure *Ulva*).

will first discuss our mechanical results, showing that the introduction of increasing quantities of *Ulva* increases the density, elastic modulus, and strength of our composites while lowering the required pressing conditions compared to pure wood self-bound boards. We will further demonstrate that the presence of *Ulva* increases the resistance to water submersion and induces flame retardant properties. Then, we will show that under the right pressing conditions, *Ulva* can be used as an alternative adhesive agent to bind pieces of wood-*Ulva* particleboards together. Finally, we provide insights into the environmental benefits of using *Ulva* seaweed as a natural adhesive in the wood-*Ulva* composites, providing an estimate of the carbon dioxide (CO<sub>2</sub>) removal potential.

## Results

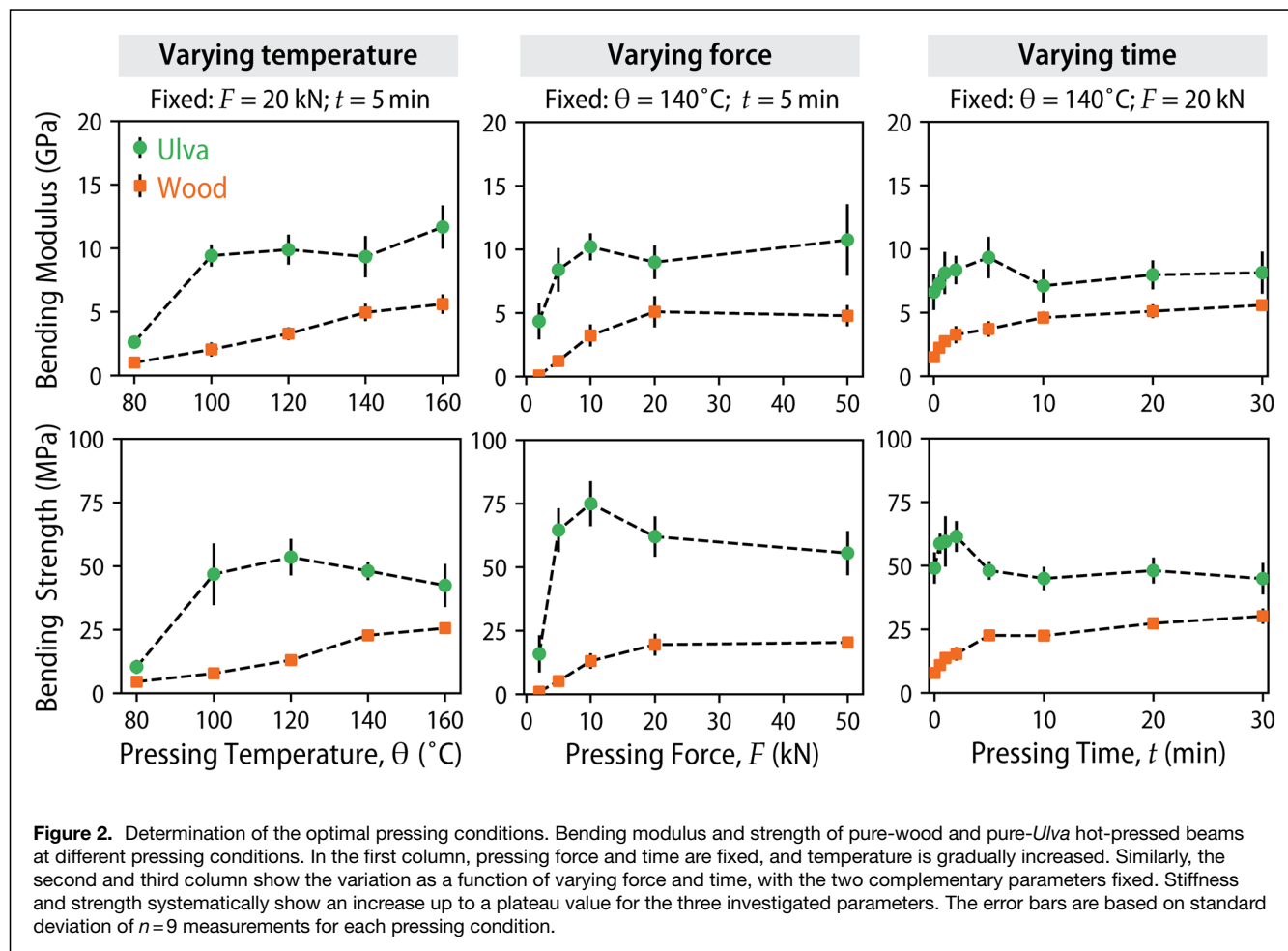
### Hot-pressing process optimization

In an effort to fabricate strong biocomposites using optimal hot-pressing conditions, we first investigated the effect of hot-pressing parameters on the mechanical performance of pure wood and pure *Ulva* beams. The hot-pressing parameters are defined by temperature of the platens compressing the mold,  $\theta$  (ranging from 80 to 160°C), the pressing force,  $F$  (ranging from 2 to 50 kN), and the pressing time,  $t$  (ranging from 0 s to 30 min). More details about the fabrication are provided in the “Materials and Methods” section. In **Figure 2**, we report the bending modulus and strength characterized using three-point bending. Each column corresponds to a fixed pair of pressing parameters, and the remaining parameter is set to vary. First, we observe that pure *Ulva* is systematically stiffer and stronger than pure wood at given pressing conditions. A

similar trend in pure *Ulva* is observed for the modulus and strength, across the different varying parameters: increasing the intensity of the pressing conditions (by either increasing temperature, pressing force, or time) initially induces a stiffening and strengthening effect, up to a maximal modulus and strength level, at which the value reaches an apparent plateau. We observe that pure-wood samples reach this plateau at higher values of each parameter than pure *Ulva*. Interestingly, increasing the pressing temperature continuously improves the strength of pure-wood samples, with no emerging plateau. A similar result was reported in Reference 12 where the authors showed that hot powderized kenaf core almost doubles in strength when pressed at 180°C compared to 140°C. From all of our results, the optimal pressing conditions used subsequently to press composites were chosen empirically to correspond to the lowest parameter such that pure-wood samples had reached their best (plateau) mechanical properties:  $F = 20$  kN, and  $t = 5$  min. The temperature was chosen at  $\theta = 140^\circ\text{C}$ , to keep a relatively low pressing temperature, while ensuring that the *Ulva* matrix would reach its full binding potential in composites.

### Microstructure and mechanical properties of *Ulva*-bonded wood composites

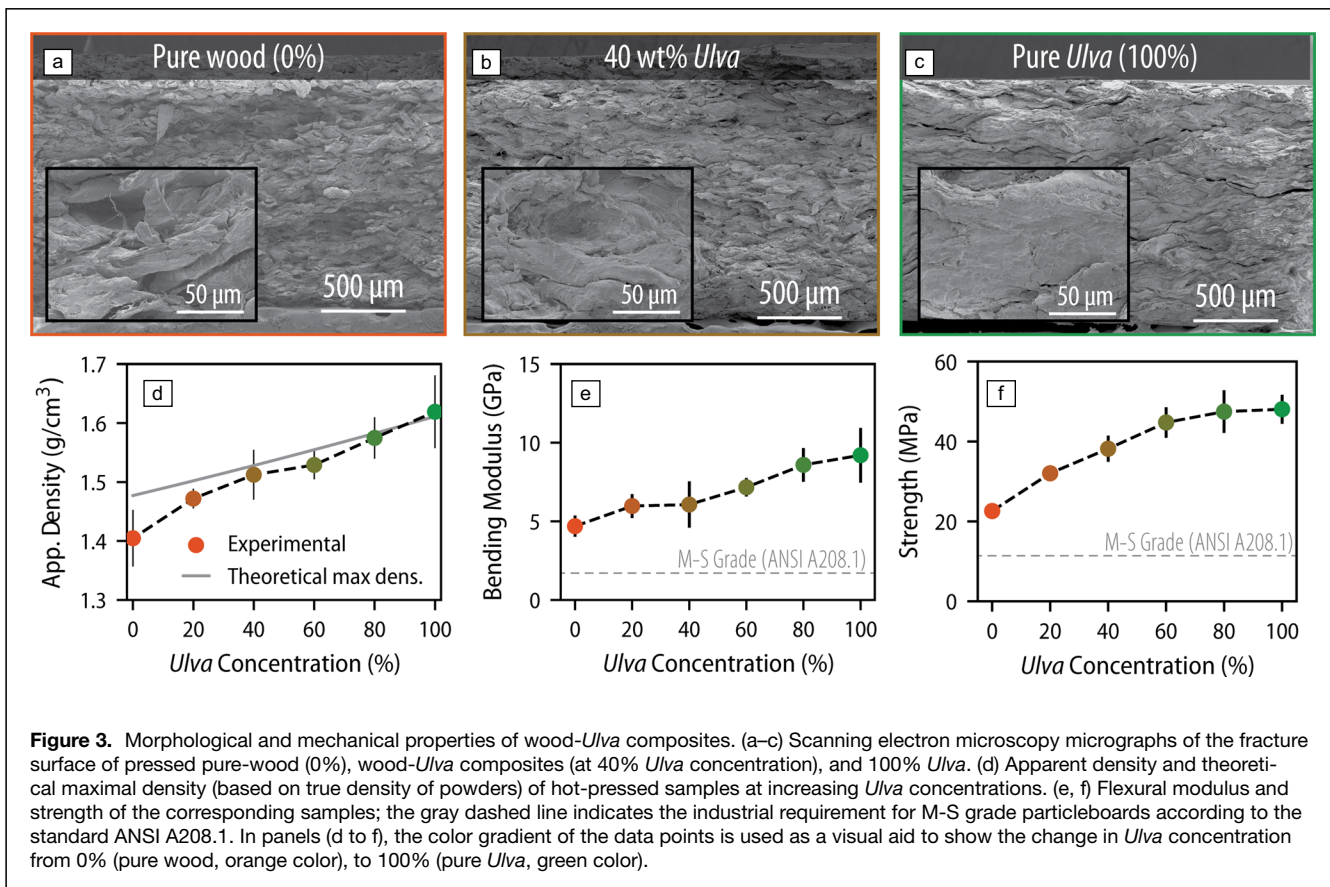
Using the optimal pressing conditions determined previously, next, we investigate the morphological and mechanical properties of wood-*Ulva* biocomposites. In **Figure 3a–c**, we provide scanning electron microscopy (SEM) images of the fracture cross section of hot-pressed samples of pure wood (0%), wood-*Ulva* (40 wt% *Ulva* content), and pure *Ulva* (100%). The pure-wood sample is heterogeneous, with



gaps between the fibers constituting the wood powder. At 40% and 100% *Ulva* concentrations, we no longer observe gaps between fibers, suggesting that the *Ulva* acts as a flowing matrix upon hot-pressing, filling the gaps between wood particles in the 40% sample. This hypothesis is further confirmed by the characterization of the apparent density of the wood-*Ulva* biocomposites at increasing *Ulva* concentrations.

In Figure 3d, the experimentally measured apparent density is compared to the theoretical maximal density, defined by the rule of mixtures as the linear combination of the respective true densities of both pure-wood and pure-*Ulva* powders (measured independently using a gas pycnometer; see the “Materials and Methods” section). The apparent density of pure-wood samples is significantly lower than the true density of its constituting powder (true density of wood powder:  $1.477 \pm 0.001$  g/cm<sup>3</sup>), suggesting the presence of gaps in the material. This difference between apparent and true density decreases for increasing *Ulva* concentration, indicating again that the *Ulva* acts as a matrix, flowing between and filling the wood-particle gaps upon thermomechanical processing. Indeed, similar apparent and true densities indicate the absence of gaps (i.e., a continuous material [true density of *Ulva* powder:  $1.661 \pm 0.002$  g/cm<sup>3</sup>]). It

should however be noted that despite being continuous, pure *Ulva* samples are not perfectly homogenous, as highlighted by the flaky regions and cracks shown in the SEM micrograph in Figure 3c. Despite these nonuniformities, which result from the tissue-level structure of *Ulva* and the fact that no severe preprocessing such as sonication was used to homogenize the biomass, the increasing degree of continuity with the introduction of *Ulva* suggests increases in overall cohesion, thus improving the mechanical properties of the resulting composites. The evolution of bending modulus and strength as a function of *Ulva* concentration (0–100% *Ulva* concentration) reported in Figure 3e–f supports this conclusion; the gradual increase of *Ulva* concentration induces an improvement of both mechanical properties. While the bending modulus seems to increase linearly with *Ulva* concentration, the strength increase shows a plateauing behavior. This nonlinear plateauing increase can be quantified by comparing relative increases in strength at different *Ulva* concentrations. The incorporation of 40 wt% *Ulva* causes an increase from 22.6 MPa (pure wood) to 38.2 MPa for the 40% composite, corresponding to an increase of 0.4 MPa/wt% *Ulva*. On the other hand, the strength then increases from 38.2 to 48.1 MPa at 100% *Ulva* (i.e., an increase of



only 0.25 MPa/wt% *Ulva*). The nonlinear strength increase could be linked to the filling behavior of the pressed *Ulva* powder between the gaps of the wood particles. At low concentrations, small amounts of *Ulva* could cause a significant improvement because they enable a drastic shift in the morphology (from discontinuous to continuous). These results show the potential for *Ulva* to act as a strengthening adhesive in wood-particle-based materials.

### Spectroscopic analyses of *Ulva*-bonded wood composites

To gain insights into the bonding changes as a result of the processing of our composites, we conducted Fourier transform infrared (FTIR) spectroscopy and x-ray photoelectron spectroscopy (XPS) studies. Our FTIR measurements focused on comparing pressed wood-*Ulva* biocomposites to pure wood and *Ulva* (Supplementary information [SI] Figure S1). As greater concentrations of *Ulva* are added to pure wood, the obtained FTIR spectra appear to change proportionally, and exhibit features indicative of the pure *Ulva* spectrum. The gradual transition of the spectral contour between the two pure states and the lack of “new” spectral features suggests that the biocomposite spectra obey the rule of mixtures and do not undergo emergent bond formation. In addition to the evaluation of the biocomposite spectra, in **Figure 4a**, we also report the FTIR spectra of pure wood and pure *Ulva* both before and

after hot-pressing (peak assignment for the powders is available in SI Table I and Table II).

Interestingly, when comparing the powders of pure wood and *Ulva* with their pressed counterparts, we do not observe any major differences in the spectra, suggesting that hot-pressing does not lead to changes in the chemical bonding within the samples. It should be noted, however, that both in wood and *Ulva*, the peaks associated with linear C–H<sub>x</sub> vibrational modes (around 2930 cm<sup>-1</sup>) become sharper and more pronounced after pressing. We observe the presence of those distinct peaks in the composites as well. This increased intensity could be explained by the melting, phase separation, and preferential flow of mobile lipids, with aliphatic tails, toward the surface of wood and *Ulva* specimens during pressing.<sup>34</sup>

XPS was also utilized to study bonding interactions during hot-pressing and composite fabrication to supplement the analysis of FTIR spectra. In **Figure 4b**, the deconvoluted C1s XPS spectra of pure wood and *Ulva* powder are compared to the corresponding hot-pressed materials. The subpeak locations of the wood spectra (approximately 285.0 eV, 286.5 eV, 287.9 eV, and 289.0 eV, respectively) agree with previous studies of wood and are therefore attributed to C–C/C–H, C–O, C=O/O–C–O, and O–C=O bonding.<sup>35,36</sup> The *Ulva* C1s spectra feature similar subpeaks associated with bonding in organic materials attributed to C–C/C–H, C–O/C–N,

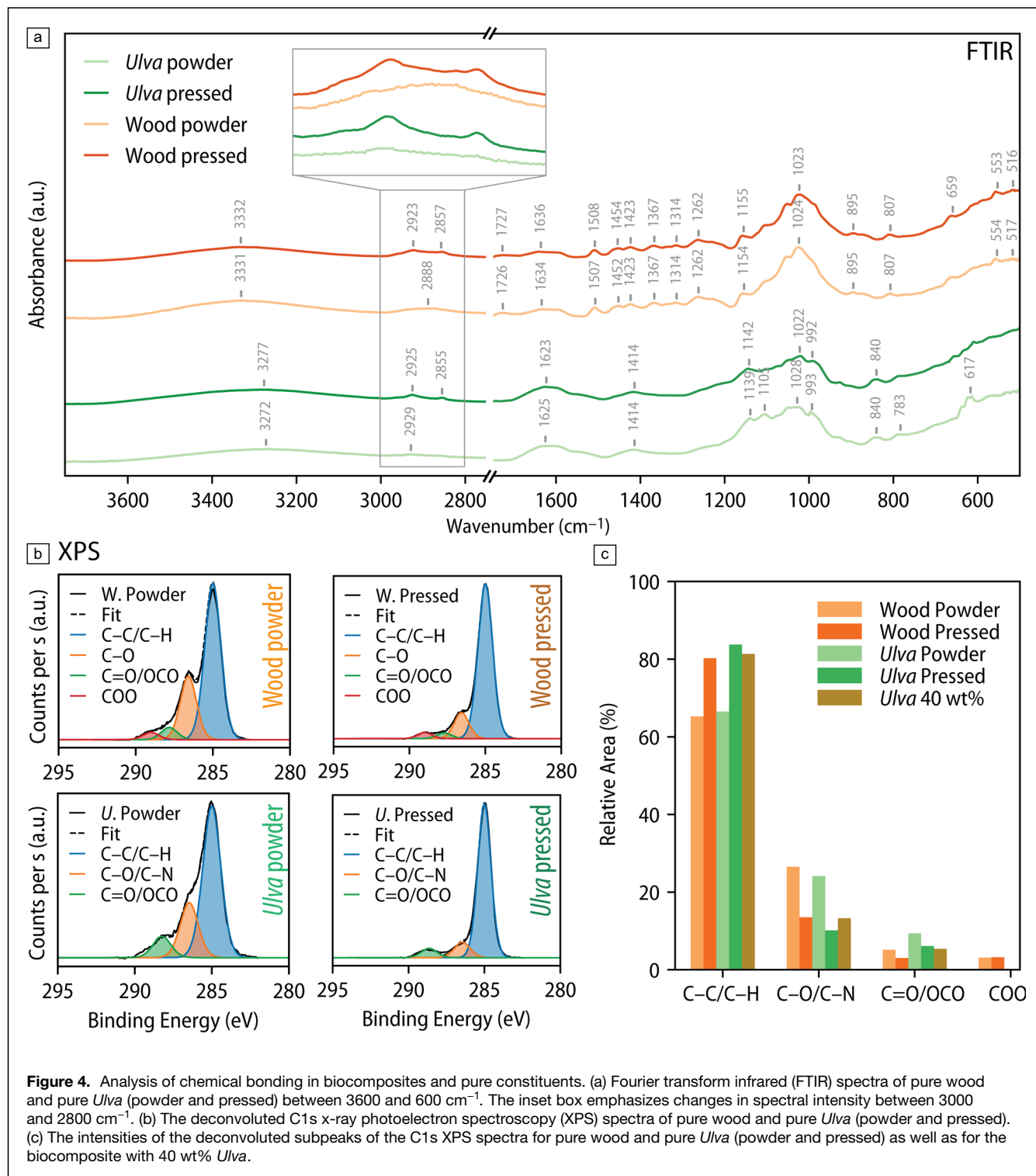


**Figure 4.** Analysis of chemical bonding in biocomposites and pure constituents. (a) Fourier transform infrared (FTIR) spectra of pure wood and pure *Ulva* (powder and pressed) between 3600 and 600 cm<sup>-1</sup>. The inset box emphasizes changes in spectral intensity between 3000 and 2800 cm<sup>-1</sup>. (b) The deconvoluted C1s x-ray photoelectron spectroscopy (XPS) spectra of pure wood and pure *Ulva* (powder and pressed). (c) The intensities of the deconvoluted subpeaks of the C1s XPS spectra for pure wood and pure *Ulva* (powder and pressed) as well as for the biocomposite with 40 wt% *Ulva*.

and C=O/O-C-O.<sup>37</sup> The intensities of the C1s subpeaks of the powder and hot-pressed wood and *Ulva*, as well as the 40 wt% *Ulva* biocomposite, are plotted in Figure 4c. We first observe that the intensities of the 40 wt% *Ulva* biocomposite subpeaks are similar to those of the hot-pressed wood and *Ulva*. This suggests similar bonding motifs are present in both

the biocomposites and the hot-pressed wood and *Ulva*. It is also evident that the pressed *Ulva* and wood samples have higher relative quantities of C-C/C-H bonding than the wood and *Ulva* powders. This observation agrees with the increased intensity observed at ~2930 cm<sup>-1</sup> in the FTIR spectra. Preferential migration of a mobile lipid phase away from the center



of the specimen during hot-pressing would explain these corresponding observations.<sup>38</sup> However, it is important to note that the increase in FTIR and XPS intensity related to C–H bonding could also be the result of contamination due to the deposition of adventitious carbon on specimen surfaces prior to spectral collection.<sup>39,40</sup> Overall, we do not observe any chemical bonding changes between the mixed components, suggesting that physical interactions rather than chemical could be the primary cohesion conferring mechanisms.

### Water stability

Although a mechanistic understanding of wood-*Ulva* biocomposite micromorphology and adhesion can help to improve iterative design of this novel system, it is also useful to evaluate the potential for direct application of *Ulva* as a particle-board adhesive. In practical settings, wood boards are often exposed to humid or even wet environments. In this section, we set out to investigate the effect of water exposure on bending strength of our wood-*Ulva* composites. As presented in **Figure 5a**, the pressed beams were first submerged and left to soak in a water bath for a defined time, before being mechanically tested. The evolution of the strength of pure wood, pure *Ulva*, and commercial medium density fiberboard (MDF) samples (serving as a control) is represented in **Figure 5b** (data points). As soaking time is increased, the strengths of pure wood and pure *Ulva* samples first decrease rapidly, before a complete loss of structural integrity is observed, where the strength drops to zero. At this point of zero strength, the samples no longer sustain their own weight and crumble apart spontaneously when retrieved from the water bath. On the other hand, while at first the MDF samples also rapidly lose strength for increasing soaking times, they reach a stationary nonzero strength after long times (tested up to 1 h). The favorable long-term water resistance of MDF can likely be attributed to the synthetic adhesives used to bind these boards. Although the composition of MDF control boards was not disclosed by the vendor, literature reports that urea formaldehyde (UF), phenol-formaldehyde (PF), and melamine-formaldehyde (MF) are the most common adhesives in MDFs. UF, PF, and MF resins, upon curing, create a significant water-resistant barrier in wood-based panels.<sup>1,41</sup>

To characterize the strength evolution more quantitatively, the time-dependent strength data were fitted using an exponential decay of the form:

$$\sigma = (\sigma_f - \sigma_0) \cdot \left( 1 - \exp\left(-\sqrt{\frac{t}{\tau}}\right) \right) + \sigma_0. \quad 1$$

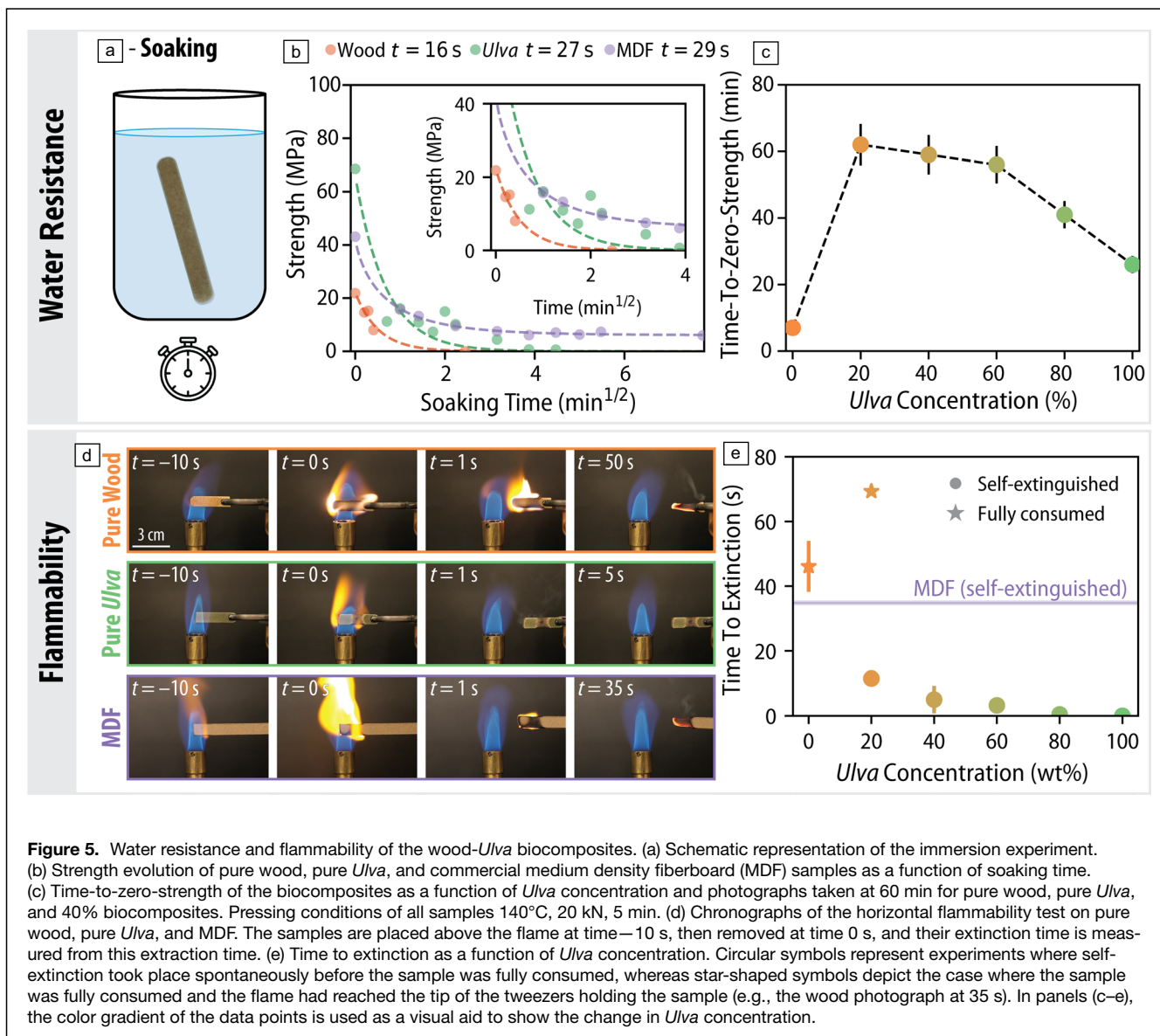
The initial strength,  $\sigma_0$ , corresponds to the dry strength of the samples, while  $\sigma_f$  is the final strength (stationary strength). The value of  $\sigma_f$  was forced to be 0 for pure wood and pure *Ulva* samples, as they were observed to reach a zero-strength in a finite time. The parameter  $\tau$  represents the characteristic decay time from  $\sigma_0$  to  $\sigma_f$  and enables a quantification of the speed at which strength is affected by water. Note that the use

of a square root for inside the exponential term is employed to account for the diffusive behavior of water seepage inside the tested samples. Although further experiments would be necessary to provide additional insights into the strength evolution and enable more precise modeling, the characteristic time offered by the proposed model allows for a comparison between materials. Pressed wood exhibits a typical strength decay time of 16 s, while *Ulva* samples decay in 27 s. The slower time evolution of *Ulva* deterioration could be attributed to the formation of a continuous matrix, and higher apparent density, upon hot-pressing, thereby slowing the diffusion of water into the samples. Interestingly, even though MDF shows a long-term nonzero strength, the initial strength drop happens at a rate only slightly slower than the pure *Ulva* samples, with  $\tau = 36$  s. This relatively rapid ingress of water can be explained by the high porosity of the commercial MDF, enhancing the wicking when immersed in water (the apparent density of the MDF was measured to be  $0.742 \pm 0.031$  g/cm<sup>3</sup>, corresponding to a porosity of 0.5 if we account for a typical true density of wood of 1.477 g/cm<sup>3</sup> as we measured experimentally).

Finally, to assess the water resistance of wood-*Ulva* composites, we quantified the time-to-zero-strength of biocomposites when immersed in water. Instead of measuring the strength at different times as described previously, in this experiment, samples were left to soak in a water bath, and extracted with tweezers regularly. The time-to-zero-strength was defined as the soaking time after which the samples would break under their own weight upon extraction from the bath. The results are provided in **Figure 5c**. Strikingly, the composites perform much better than their pure counterparts. As an example, the biocomposite sample with the best water resistance (containing 80 wt% wood and 20 wt% *Ulva*) remained structurally resistant for 59 min as opposed to 7 min for pure wood and 26 min for pure *Ulva*. Visually, the failure mode of pure wood and pure *Ulva* were slightly different; pure-wood samples disaggregated and crumbled apart, while pure *Ulva* samples swelled and displayed a gel-like structure. The non-linear behavior of time-to-zero-strength as a function of *Ulva* concentration could be attributed to the formation of a dense matrix of *Ulva* in the composites as described previously (see **Figure 3d**). This compact matrix could slow down the diffusion of water inside the samples, thereby temporarily shielding the wood particles from exposure to water and delaying their disaggregation. To enable load resistance of such composites when soaked, further research is still needed.

### Flammability

Similar to water resistance, resistance to flammability is an essential characteristic of wood panels applied as construction materials. Synthetic additives are often incorporated in wood-based fiberboards to increase the flame resistance, but such additives are often unsustainable and can be hazardous to human health.<sup>3</sup> To assess the flame retardance of our biocomposites, we measured the time to self-extinction of



pure wood, pure *Ulva*, MDF, and wood-*Ulva* biocomposite samples brought in contact with an open flame for 10 s and subsequently pulled away. In Figure 5d, we provide chronological images of the flammability experiment for pure wood, pure *Ulva*, and MDF. The times to self-extinction are reported in Figure 5e. Two distinct behaviors were observed after samples were removed from the flame. The first response observed was spontaneous self-extinction before the flame had reached the tip of the metallic tweezers holding the samples. For example, the time-lapse for pure *Ulva* in Figure 5d demonstrates self-extinction shortly after extracting the sample from the flame (1 s). This case is represented by circular symbols in Figure 5e. In the second scenario, the samples were fully consumed and extinguished only when the flame had reached the tip of the tweezers. The pure-wood sample, for instance, is totally consumed after 50 s of burning

(Figure 5d). This second case is represented by star-shaped symbols in Figure 5e.

The results show an increasing flame-retardant behavior for wood-*Ulva* biocomposites as the concentration of *Ulva* increases. The pure-wood samples (0%) systematically underwent complete combustion, thereby corresponding to the “fully consumed” category. At 20 wt% *Ulva*, one sample self-extinguished after 11.5 s, and another was fully consumed after 69.3 s. At higher *Ulva* concentrations ( $\geq 40$  wt%), samples are exclusively self-extinguished, with extinction times decreasing from 5 s for the 40% sample to 0 s for pure *Ulva* samples, corresponding to an immediate extinction upon withdrawal from the flame. The increased resistance to flammability could be explained by differences in the chemical composition of wood and *Ulva*. First, our ash-content measurements (see the “Materials and Methods” section) show





that *Ulva* seaweed has a significantly higher concentration of inorganic, noncombustible matter than Douglas fir. Indeed, as presented in SI Figure S2a, the ash content of our *Ulva* was measured at  $34.8 \pm 0.6$  wt% by dry weight (similarly to values reported in literature<sup>42</sup>), revealing the high content of inorganic components such as potassium, sodium, or chloride. In comparison, the ash content of the wood was measured at only  $0.6 \pm 0.02$  wt% by dry weight (comparable to values reported in Reference 43) (see SI Figure S2a). This difference in ash content alone could explain the difference in flammability between wood and *Ulva*. Differences in flammability could also be partially attributed to differences in the concentration of protein and phosphorus within the two biomasses.<sup>44</sup> As protein is the major source of nitrogen in most biomass, nitrogen and protein contents are often considered interconvertible (protein content = N\*6.25).<sup>45</sup> Using this method, we quantified the protein content of *Ulva* to be higher than wood (see SI Figure S2b). The amount of phosphorus in two species of *Ulva* ( $\sim 2500$   $\mu\text{g/g}$ )<sup>46</sup> is also recorded to be approximately two orders of magnitude higher than that of Douglas fir wood ( $\sim 40$   $\mu\text{g/g}$ ).<sup>47</sup> The presence of proteins and phosphorus are believed to encourage the formation of phosphoric acid and therefore accelerate protective charring during combustion. Irrespective of the mechanism, the attractive natural flame retardance of *Ulva* biomass encourages its application as an alternative to formaldehyde resins for wood panel adhesion.

### ***Ulva* powder as an adhesive agent between two prepressed beams**

The ability to adhere wood panels together (e.g., using glues) is an important capability to ensure design flexibility in construction materials. In this section, we consider the use of pure *Ulva*, rather than synthetic glues, to attach two of our beams together (respectively using two beams of pure wood and wood-*Ulva* biocomposites of 40 wt% *Ulva*). The term adhesive agent will be used in this section, not to be confused with the adhesives used in wood particleboards to bind the particles together and provide cohesion. To quantify the strength of pure *Ulva* powder as an adhesive agent, we hot-pressed a thin layer of *Ulva* powder between two prepressed beams. The fabrication steps of this “sandwiched” configuration are described in Figure 6a and detailed in the “Materials and Methods” section. A typical hot-pressed and adhered stack is presented in Figure 6b, highlighting the presence of a thin layer of *Ulva* between the two prepressed beams. In order to quantify the binding strength of the hot-pressed *Ulva*, the shearing strength of the adhered stacks was tested using a custom-made grip in a mechanical test frame as described in Figure 6c. Shouldered grips were used to induce pure shear along the *Ulva* adhesion plane. The corresponding shear stress upon failure (which consistently occurred along the *Ulva* plane) was recorded and the corresponding values are reported in Figure 6d. Both for the pure wood and the 40 wt% biocomposite prepressed beams, these results are compared to two other methods. First, the “Bulk” denomination refers to the baseline shear strength of

a single thick beam composed entirely of the same material (either pure wood, or a 60–40 wt% wood-*Ulva* composition). To ensure comparable results, the thickness of these thick uniform beams was chosen to be twice that of the beams composing the stacked configuration. Second, the “Super Glue” provides a comparison with another gluing method between two prepressed beams using a commercial super glue serving as a control.

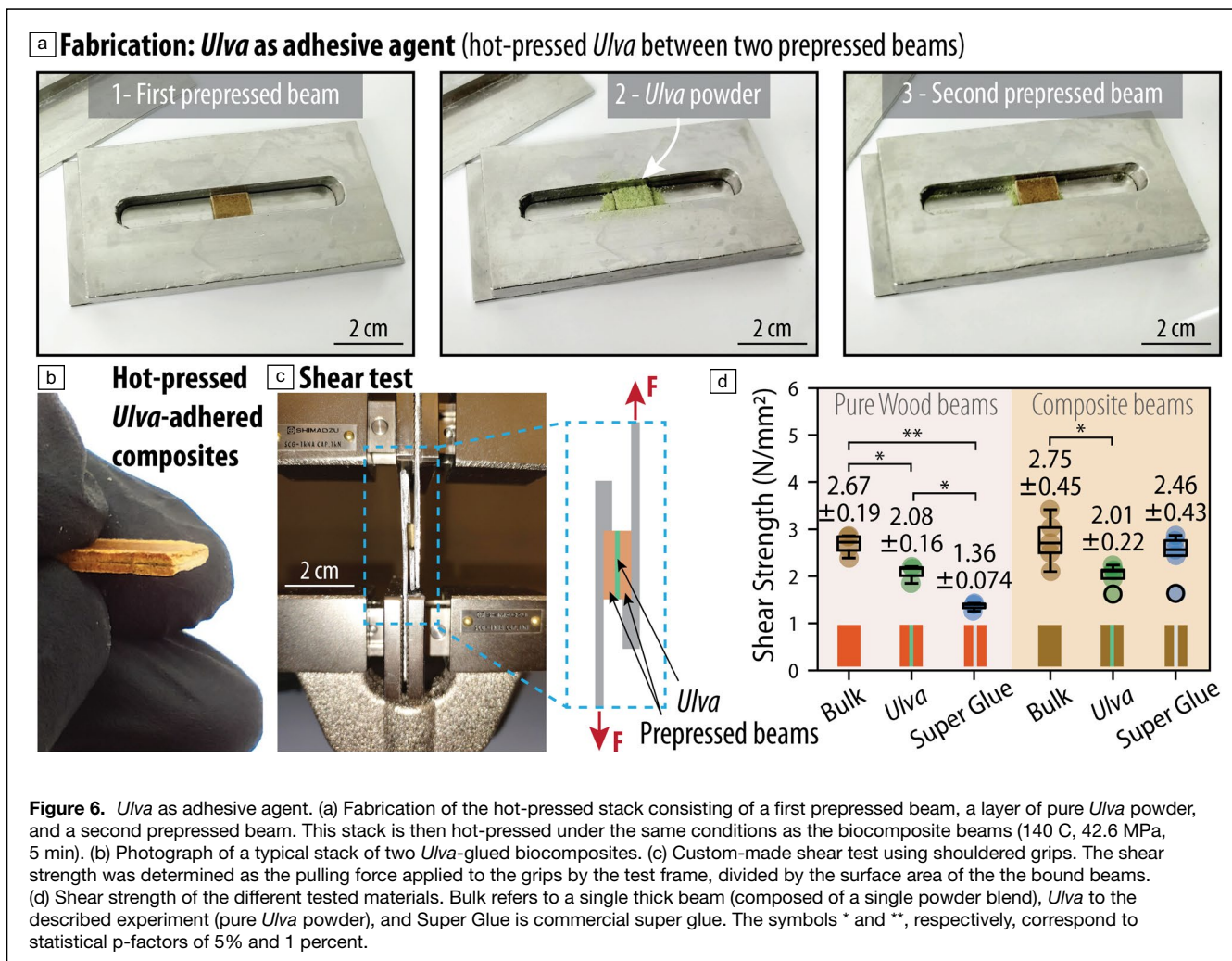
We first discuss the results corresponding to the pure wood beams attached together (left side of Figure 6d). Unsurprisingly, the bulk beam has a shear strength higher than the *Ulva*- and super glue adhered stacks, as the bulk part does not possess a discontinuous interface. Interestingly, *Ulva* provides significantly stronger adhesion properties than the super glue (shear strength of  $2.08 \pm 0.16$  compared to  $1.36 \pm 0.074$  N/mm<sup>2</sup>). In the case of the prepressed biocomposite beams (right side of Figure 6d), the bulk piece again possesses the highest shear strength, while the *Ulva* and super-glue bound beams show statistically similar strengths ( $2.01 \pm 0.22$  versus  $2.46 \pm 0.43$  N/mm<sup>2</sup>).

In conclusion, pure *Ulva* powder enables the strong adhesion of two of our wood-*Ulva* biocomposite panels when subjected to the right hot-pressing conditions, with strengths similar to the ones achieved using a commercial super glue. This experiment highlights the flowing behavior of pure *Ulva* upon hot-pressing, leading to a continuous matrix that enables the secure attachment of two wood panels together.

### **Environmental assessment**

In addition to the benefits of *Ulva* adhesive on the materials properties of wood composites, there are also environmental benefits throughout the life cycle of the product in comparison to current market alternatives. The majority of commercial wood particleboards use formaldehyde-based synthetic resins as binders.<sup>48,49</sup> Formaldehyde is known to be toxic<sup>50</sup> and as such, there is significant interest in safer, bio-based alternatives (e.g., see References 51–56). To be an acceptable replacement, environmentally friendly alternative binders must have adequate physical properties, such as strength, flame retardancy, and water resistance, as well as economic incentives including ease of acquisition, straightforward manufacturing, and competitive pricing.

Life-cycle analysis (LCA) is used to compare environmental benefits and detriments across a production life cycle and identify particular hot spots, or areas for improvement, as well as compare similar products or processes.<sup>57</sup> The scope of a LCA can be cradle-to-gate, ending analysis with a completed product to be sold, or cradle-to-grave, which considers the end of life of the completed product. For any product claiming a carbon benefit, a cradle-to-grave scope is needed to avoid overestimating the benefit of carbon removed<sup>58,59</sup> as well as to consider biodegradability or recycling of components. Multiple categories are used in LCA to assess different environmental aspects of a process, including the resources used, energy consumed, emissions generated (usually reported in terms of global warming



potential, GWP, which also usually includes carbon removal), and toxicity (to human health or environment). At this time, conducting a complete LCA for the development of *Ulva*-wood composites is not warranted as this is a research-scale project, without an established manufacturing process. The current scale of fabrication makes it infeasible to accurately assess emissions generation, carbon removal, or even cost. As commercial pathways are explored, a complete LCA is recommended for future work to streamline the process to improve environmental aspects as well as provide a standardized assessment to be able to compare this product with others on the market and include in an Environmental Product Declaration.

Despite this impediment to formal analysis, the inclusion of *Ulva* in wood composites has several environmental impacts that are worth discussing. Seaweeds like *Ulva* can be grown naturally or aquacultured and provide habitat to aquatic species, regulate the levels of carbon and nutrients, and further contribute to the health of the ecosystem in their surroundings.<sup>32,60–62</sup> Seaweed is also faster growing than wood and easier to cultivate. Hot spots in the LCA for other bio-based composite materials have been noted for energy consumption

in the processing phase, including in the drying of the raw material<sup>63</sup> as well as for the hot-pressing.<sup>52,64</sup> The energy required to grind down the biological materials into powders can also contribute to the overall CO<sub>2</sub> emissions.<sup>65</sup> Other factors that influence the overall climate impacts of the process that would be assessed in a full LCA include the distance seaweed and products are transported, established processes for reuse or recyclability in a circular economy,<sup>66,67</sup> the scale and size of construction wood panels and associated manufacturing apparatus, and any changes to sourcing of wood or seaweed due to increase in operation scale.<sup>68</sup> The composite itself is also biodegradable, while MDF and particleboard panels are extremely challenging to recycle and as a result are most often landfilled or burned for heat value after usage.<sup>69</sup>

### CO<sub>2</sub> sequestration estimate

Although a formal LCA of our biocomposites cannot yet be conducted, a preliminary estimation of the CO<sub>2</sub> sequestration potential can be provided. *Ulva* species have one of the highest carbon capture capacities among seaweeds,<sup>70,71</sup> ranging around 14–50 mg C per g of dry *Ulva* per day, with



**Table I. CO<sub>2</sub> sequestration potential of wood-*Ulva* biocomposites as a function of composition.**

<i>Ulva</i> Content in Wood- <i>Ulva</i> Biocomposite (wt%)	Potential for CO <sub>2</sub> Sequestration (kg CO <sub>2</sub> /kg composite)
0	1.71
20	1.46
40	1.21
60	0.96
80	0.71
100	0.47

a 23.9 wt% carbon content as measured experimentally (see SI Figure S2b and the “Materials and Methods” section for carbon and nitrogen characterization). This carbon content corresponds to a CO<sub>2</sub> sequestration of raw *Ulva* of 0.88 kg CO<sub>2</sub>/kg dry *Ulva*. This advantageous carbon sequestration is, however, reduced by the CO<sub>2</sub> emissions associated with the steps necessary to attain the dry *Ulva* powder used in this study. Koesling et al.<sup>72</sup> attempted to provide an estimate of the CO<sub>2</sub> emissions associated with the cultivation and drying of another macroalgae, sugar kelp. In their proposed ideal scenario relying on hydrothermal electricity from the Norwegian grid, they account for seeding, deployment, harvesting, transport and storage, and drying, and report CO<sub>2</sub> emissions of 0.41 kg CO<sub>2</sub>/kg dry seaweed. Taking the carbon sequestration into account, this method corresponds to an estimated net negative emission of  $\mu_{Ulva} = -0.47$  kg CO<sub>2</sub>/kg dry *Ulva*. On the other hand, wood typically has a carbon content of 46.7 wt%. (see SI Figure S2b), translating into a negative emission of  $\mu_{Wood} = -1.71$  kg CO<sub>2</sub>/kg dry wood neglecting potential CO<sub>2</sub> emissions from the mechanical grinding to reduce particle size (note that negative emissions correspond to a sequestration). We can estimate the CO<sub>2</sub> removal potential of the wood-*Ulva* composites using a rule of mixtures:

$$\mu_{Composite} = c_{Ulva} \cdot \mu_{Ulva} + (1 - c_{Ulva}) \cdot \mu_{Wood}, \quad 2$$

where the notation  $\mu$  corresponds to the specific CO<sub>2</sub> emissions of each constituent, and  $c$  corresponds to the relative weight concentrations of the components. In Table I, we apply this formula to calculate the potential for CO<sub>2</sub> sequestration for different *Ulva* concentrations in the biocomposites. For example, the 40 wt% *Ulva* composite would enable a carbon sequestration potential of 1.21 kg CO<sub>2</sub>/kg composite.

We note that this is merely an estimate that excludes the carbon cycling that occurs while the seaweeds are growing that could potentially export more carbon to permanent sinks, as well as ignores the temporal aspect of carbon removal that is needed for climate benefits. The permanence of carbon removal will ultimately depend of the lifetime of the product and carbon cycling in growth,<sup>62</sup> and will need to be appropriately quantified before claiming or monetizing these benefits.<sup>58,73</sup> As a means of comparison, the specific CO<sub>2</sub> emission of solid urea formaldehyde was quantified

in a LCA performed by Bushi et al.,<sup>74</sup> where they reported  $\mu_{UF} = +1.53$  kg CO<sub>2</sub>/kg solid UF, a value significantly higher than the (negative) value for *Ulva*. At a typical UF concentration for commercial particleboards (comm. PB) in the range 7–10 wt%,<sup>75</sup> using Equation 2 with our value of  $\mu_{wood}$  (and replacing  $\mu_{Ulva}$  with  $\mu_{UF}$ ), we find the typical CO<sub>2</sub> sequestration:  $-\mu_{comm.PB} = [1.39, 1.48]$  kg CO<sub>2</sub>/kg comm. PB, in the same range as the sequestration potential of the 20% wood-*Ulva* composite. Note that even though the specific CO<sub>2</sub> sequestration potentials are in the same order of magnitude between wood-*Ulva* composites and commercial particleboards, the potential for recycling and composting makes up for a major advantage for all-bio-based composites.

Our *Ulva*-wood composites are to be considered medium-term carbon sinks, as the carbon could be durably stored in the product for tens of years, before likely being released during biodegradation. In this product, *Ulva* most likely represents a similar carbon removal potential as pure wood materials,<sup>68</sup> though the cultivation process is much more rapid, weeks as opposed to decades. Compared to other macroalgae such as kelp, *Ulva* has not been documented to export carbon to the deep sea for permanent burial (e.g., see References 76 and 77), due to its typical growth on rocky areas in the intertidal.

Importantly, even if there are no additional carbon sequestration benefits to using seaweed instead of pure wood, there are additional environmental and social benefits that can be achieved. Using seaweed as a binder instead of urea formaldehyde greatly reduces the toxicity of the wood panels, which is seen as the primary benefit without compromising product quality. *Ulva* cultivation is relatively inexpensive<sup>25</sup> and is more accessible to women and gender minorities,<sup>78,79</sup> who have typically been excluded from industrial timber harvest and processing.<sup>80</sup> These benefits, while cautiously estimated here, can only be accurately assessed as the processing technology transitions from TRL 0 to pilot scale.

## Discussion and conclusion

There is an urgent need to provide alternatives to synthetic binders such as formaldehyde-based adhesives to mitigate the environmental impact of wood particle- and fiberboards. While a wide variety of solutions are proposed and investigated, including leveraging self-binding of pure lignocellulosic materials under heat and pressure, or using bio-based adhesives, the success of these methods often relies on significant preprocessing steps. In this article, we have introduced wood-*Ulva* biocomposites, where the untreated *Ulva* powder plays the role of binding and densifying matrix between the lignocellulosic wood particles, enabled by *Ulva*'s flowing behavior upon hot-pressing. After determining the optimal pressing parameters on pure wood and pure *Ulva* samples, we have assessed the morphological and mechanical properties of biocomposites of varying wood-*Ulva* concentrations. Our results show that the



porosity of our biocomposites rapidly decreases as the *Ulva* concentration increases, concurrently with improving mechanical properties (strength and stiffness). Based on spectroscopy methods (FTIR and XPS), we hypothesized that fatty acids could migrate upon hot-pressing, as suggested by the higher relative quantities of C–C/C–H bonding in pressed samples, compared to the unpressed raw powders, while no chemical bond changes were observed upon processing.

We further performed experiments to assess the viability of our method in the context of applications. We characterized our wood-*Ulva* biocomposites by testing their water and flame resistance and assessed the possibility of using pure *Ulva* powder as an alternative to synthetic glues when attaching particleboards together. When submerged in water, the samples consistently showed a complete loss of mechanical integrity after some time. Interestingly, however, wood-*Ulva* composites showed better water resistance than their pure-constituent counterparts. For example, the samples with 20 wt% *Ulva* concentration remained structurally stable for an average of 59 min, compared to 7 and 26 min for pure-wood and pure-*Ulva* samples, respectively. This synergistic behavior could be attributed to the densification of the samples in the presence of *Ulva*, thereby slowing down the diffusion of water between the wood particles. Next, the presence of *Ulva* also increases the flame resistance of our biocomposites. A beam containing 40 wt% *Ulva*, after being exposed to an open flame for 10 s and then pulled away, self-extinguished spontaneously within 5 s on average, whereas, under the same conditions, pure-wood samples caught on fire until fully consumed (sample charred entirely). In the last experiment, we quantified the adhesion strength between two pre-pressed beams when bound using either hot-pressed *Ulva*, or commercial super glue. We observed that, on average, *Ulva* provides better binding properties than glue between pure wood beams, while similar binding properties were observed on the 40 wt% *Ulva* beams. These results suggest that *Ulva* powder can be used as an adhesive agent and highlight the strong bonding between wood and *Ulva* when subject to heat and pressure.

Finally, an environmental assessment of the wood-*Ulva* biocomposites was proposed. Although at this early research stage, a full LCA is not warranted as it would lack important parameters ground in industrial-scale processes, several benefits of using *Ulva* seaweed in wood-*Ulva* biocomposites were highlighted. In addition to providing a healthy aquatic environment by regulating carbon levels and nutrients in its ecosystems, *Ulva* can also act as a carbon sink by capturing CO<sub>2</sub> when growing. This CO<sub>2</sub> sequestration potential was quantified for different wood-*Ulva* compositions.

In summary, wood-*Ulva* biocomposites provide an encouraging pathway toward fabricating dense fully bio-based particle and fiberboards with minimal preprocessing steps. Further research should be led to address the rapid water absorption and limited water resistance of bio-based wood particleboards, for example, by incorporating bio-based hydrophobic

additives (such as chitosan)<sup>81</sup> or cross-linking agents (such as glyoxal),<sup>82</sup> respectively.

## Materials and methods

In this section, we describe the material sourcing, fabrication, and testing methods used throughout this report to characterize the wood-*Ulva* biocomposites.

### Materials

#### *Ulva*

*Ulva* seaweed was cultivated in natural seawater, harvested, and freeze-dried for convenience by the Marine and Coastal Research Laboratory of the Pacific Northwest National Laboratory (PNNL) in indoor ponds in Sequim (Wash., USA) before being shipped. The *Ulva* was then ground up using an electric coffee grinder (Hamilton Beach Fresh Grind, Southern Pines, N.C., USA) in batches of  $10 \pm 2$  g ground for 1 min and subsequently sieved through a 297  $\mu\text{m}$  mesh to remove large particles.

#### Wood

Untreated wood sawdust (Douglas Fir, *Pseudotsuga menziesii*) was acquired as waste from the wood shop at the University of Washington (Seattle, Wash., USA) and sieved through a 150  $\mu\text{m}$  mesh to remove large particles.

#### Commercial MDF

To provide a comparison with our biocomposite samples, a commercial MDF of 2-mm-thick boards (6"  $\times$  8", purchased from Juvale) was also tested in the water stability and flammability experiments. Note that the composition of the MDF was not disclosed by the vendor.

#### True powder density and apparent sample density measurements

##### True density of powder

The true density of powders was measured using the gas pycnometer Ultrapyc 5000 (Anton Paar, Graz, Austria) using the 0.25 cm<sup>3</sup> cell. The target temperature and pressure were, respectively, set at 20°C and 10 PSI using the "Pulse" preparation mode. The reported density and uncertainty were measured as the average and standard deviation of the five last measurements before convergence was reached.

##### Apparent density of samples

The apparent density of pressed samples was characterized by the mass of the sample divided by its apparent volume as measured using the macroscopic dimensions of the samples filed down to a cubic shape. Lengths were measured with a digital caliper (0.01-mm precision).



## Sample fabrication

### Pressed beams

Blends of controlled proportions of wood and *Ulva* powder were mixed using a planetary speed mixer (SpeedMixer DAC 330–100 PRO, FlackTek, Landrum, S.C., USA) at 2500 rpm for 1 min. The resulting powder was then pressed under heat and pressure using a hot-press (TMAX-SYP-600, TMAXCN, China) into bars of  $1 \pm 0.05$  g using stainless-steel custom molds. The resulting area of the samples was 60 mm  $\times$  8 mm with rounded corners (of radius 3.5 mm) with a typical thickness of 1.50 mm. The temperatures for hot-pressing,  $\theta$ , ranged from 80 to 160°C, the pressing force,  $F$ , ranged from 2 to 35 kN (corresponding to an imposed pressure ranging from 4.3 to 74.5 MPa; 1 kN corresponds to 2.13 MPa, see SI Table III), and the pressing time,  $t$ , ranged from 0 to 30 min. A pressing time of 0 min was imposed by increasing the pressing force up to the target value, and then immediately releasing pressure. After pressing, the samples were demolded and cooled down in between two aluminum plates to ensure the straightness of the sample. Before any further testing, the samples were preconditioned for at least 24 h in a dry environment using desiccators.

### *Ulva* as binding agent between prepressed beams

The shear strength of beams bound together with hot-pressed *Ulva* was tested after fabricating samples using the following method. First, a short (prepressed) beam of determined length was inserted inside the mold that was previously used for composite fabrication. A thin layer ( $\sim 0.5$  mm) of *Ulva* powder was then sprinkled on top of this part, before an identical beam was stacked on top. The adhesive property of *Ulva* was then enabled by hot-pressing the stack at 140°C for 5 min. The applied pressing force was calibrated depending on the surface area of the two beams to ensure an equivalent pressure to the one imposed during beam hot-pressing (corresponding to a pressure of 42.6 MPa). The “sandwich” sample was then removed from the mold and left to cool down for 10 min before proceeding to the mechanical shear test.

To provide a comparison to a commercial synthetic adhesive agent, the shear strength of two beams bound together with super glue was tested. A thin layer ( $\sim 0.1$  mm) of super glue (super glue, Gorilla Glue Inc., Ohio, USA) was applied onto one prepressed beam and the second beam was then pressed on it by hand for 45 s.

### Mechanical testing

The mechanical properties of the wood-*Ulva* biocomposites were assessed through flexural three-point bending (3 PB) tests on a universal test frame (Autograph AGS-X 10kN, Shimadzu Scientific Instruments, Columbia, Md., USA). The indentation velocity was adapted to impose a strain rate of 0.5%/s in the elongated part of the tested beam. To provide multiple data points per beam, a first 3 PB test was performed on the entire beam (support length of 40 mm), and the

two resulting halves were then also tested (support length of 20 mm), thus providing three measurements per beam. This process was repeated for three entire beams to provide nine measurements per pressing condition. The force–displacement data provided by the test frame software (Trapezium X) were then post-processed in Python to extract the flexural modulus, strength, elongation to break, and toughness to fracture. No significant differences were observed between the tests of full or half beams.

### FTIR

FTIR was performed on the PerkinElmer Frontier (Waltham, Mass., USA) in attenuated total reflectance (ATR) mode over the wavenumber range 4000–400  $\text{cm}^{-1}$  with a resolution of 2  $\text{cm}^{-1}$  and 64 repetitions per measurement.

### XPS

XPS measurements were performed on an AXIS Ultra DLD (Kratos, Trafford Park, Manchester, UK) on pure wood and pure *Ulva* (in the powder and pressed state), and on a wood-*Ulva* 60:40 biocomposites (only in the pressed state). This machine has a monochromatized Al  $K\alpha$  x-ray and charge neutralization is enabled through a low energy electron flood gun. The spot size of the x-ray beam for acquisition was on the order of 700  $\times$  300  $\mu\text{m}^2$ . During spectral acquisition, the pressure inside the analytical chamber was below  $5 \times 10^{-9}$  Torr. Pass energy for survey and detailed resolution spectra (composition) was set to 80 eV. On the other hand, the pass energy for the high-resolution spectra was 20 eV. The angle between the sample normal and the input axis of the energy analyzer (takeoff angle) was 0°. High-resolution spectra were acquired in the binding energy regions of C 1 s and O 1 s for each sample. Finally, CasaXPS<sup>83</sup> was used to fit the peaks on the high-resolution spectra. A Shirley background was used, and all binding energies were referenced to the C 1 s C–C bonds at 285.0 eV.

### Flammability

The flame resistance of our samples was assessed using an adapted UL94-HB setup. Half-beams of the pressed samples were horizontally brought in contact with an open flame for 10 s (generated using a lab Bunsen burner) before being pulled away from the flame. The time to self-extinction was then recorded for each sample. A distinction was made for samples that spontaneously self-extinguished, as opposed to samples that self-extinguished once the flame had reached the tip of the tweezers holding the sample (labeled “fully consumed”).

### Water absorption

Resistance to water was characterized using an immersion experiment. The mass and dimensions of a dry beam were measured prior to fully immersing the sample in deionized (DI)



water for a controlled duration. After this period, the sample was extracted and padded on dry lab wipes to remove excess water. Samples were then weighed and measured before being tested mechanically using the method described above. Given the wide variety of resistance to water of our samples depending on composition, the first test consisted in immersing a sample (of one composition) in water to regularly probe its resistance by hand. A sample was deemed non-testable when it spontaneously crumbled under the slight pressure of the tweezers. A zero strength was attributed to this time point ( $t_{\text{end}}$ ), and the time distribution for testing was based on this final time (typically 5–10 samples were tested from 0 min to  $t_{\text{end}}$ ).

### Ash-content characterization

Homogenized biomass samples were dried in pre-ashed and tared aluminum weigh dishes at ca. 100°C overnight to remove moisture, cooled in a desiccator, weighed, and then ashed at 540°C for 2 h to remove volatile matter. After cooling, the samples were transferred to a desiccator and weighed again to determine the nonvolatile (ash) matter remaining. Ash content was calculated as a percentage of the total dry sample mass.

### Total carbon and nitrogen content characterization

Total carbon and nitrogen for wood and *Ulva* samples on a percent dry weight basis were determined from triplicate, homogenized dry samples of 5 mg using an ECS 8020 CHNS-O Elemental Analyzer (Orbit Technologies Pvt. Ltd.) as described in Reference 84. Calibration curves were created with acetanilide and atropine was used as a check standard every 10 samples.

### Author contributions

P.G., C.S., and E.R. designed research; P.G., I.R.C., H.N., R.B., and M.P. performed research; K.H. performed carbon–nitrogen characterizations; P.G., I.R.C., M.P., and E.R. analyzed experimental data; S.E. cultivated and harvested the *Ulva* seaweed; S.E., D.R., and P.G. performed the environmental assessment; P.G., I.R.C., S.E., D.R., and E.R. wrote the manuscript.

### Funding

Funding for *Ulva* cultivation provided in part by DOE-ARPA-E, Award No. 20/CJ000/09/02.

### Data availability

The data that support the findings of this study are available from the corresponding author upon reasonable request.

### Competing interests

The authors have no competing interests to declare.

### Supplementary information

The online version contains supplementary material available at <https://doi.org/10.1557/s43577-024-00734-5>.

### References

1. M.H. Hussin, N.H. Abd Latif, T.S. Hamidon, N.N. Idris, R. Hashim, J.N. Appaturi, N. Brosse, I. Ziegler-Devin, L. Chrusiel, W. Fatriasari, F.A. Syamani, A.H. Iswanto, L.S. Hua, S.S.A.O. Al Edrus, W.C. Lum, P. Antov, V. Savov, M.A. Rahandi Lubis, L. Kristak, R. Reh, J. Sedláčik, *J. Mater. Res. Technol.* **21**, 3909 (2022)
2. N. Laemsak, M. Okuma, *J. Wood Sci.* **46**, 322 (2000)
3. A.H. Khoshakhlagh, M. Mohammadzadeh, S.S. Manafi, F. Yousefian, A. Gruszecka-Kosowska, *Environ. Pollut.* **331**, 121854 (2023)
4. H. Hassannejad, A. Shalbanaf, M. Rahmaninia, *J. Adhes.* **96**, 797 (2020)
5. R. Jazayeri, S.K. Najafi, H. Younesi, *Int. J. Adhes. Adhes.* **126**, 103448 (2023)
6. W.H. Mason, Process of making integral insulating board with hard welded surfaces, US Patent 1812969A (July 1931)
7. E. Oliyai, F. Berthold, L.A. Berglund, T. Lindström, *ACS Sustain. Chem. Eng.* **9**, 1899 (2021)
8. T. Joëlsson, G. Pettersson, S. Norgren, A. Svedberg, H. Höglund, P. Engstrand, *Nord. Pulp Pap. Res. J.* **35**, 195 (2020)
9. J.E. Jakes, C.G. Hunt, S.L. Zelinka, P.N. Ciesielski, N.Z. Plaza, *Forests* (Basel) **10**, 1084 (2019)
10. J. Xu, R. Widyorini, H. Yamauchi, S. Kawai, *J. Wood Sci.* **52**, 236 (2006)
11. K.C. Shen, Method of making composite products from lignocellulosic materials, US Patent 5017319A (May 1991)
12. N. Okuda, M. Sato, *J. Wood Sci.* **50**, 53 (2004)
13. S. Suzuki, H. Shintani, S.-Y. Park, K. Saito, N. Laemsak, M. Okuma, K. Iiyama, *Holzforchung* **52**(4), 417 (1998)
14. X. Yang, M.S. Reid, P. Olsén, L.A. Berglund, *ACS Nano* **14**, 724 (2020)
15. M. Hazwan Hussin, N.A. Samad, N.H.A. Latif, N.A. Rozuli, S.B. Yusoff, F. Gambier, N. Brosse, *Int. J. Biol. Macromol.* **113**, 1266 (2018)
16. J. Li, Y. Lyu, C. Li, F. Zhang, K. Li, X. Li, J. Li, K.-H. Kim, *Int. J. Biol. Macromol.* **227**, 1191 (2023)
17. F. Pichelin, C. Kamoun, A. Pizzi, *Holz Roh Werkst.* **57**, 305 (1999)
18. M. Jimenez Bartolome, N. Schwaiger, R. Flicker, B. Seidl, M. Kozich, G.S. Nyanhongo, G.M. Guebitz, *N. Biotechnol.* **69**, 49 (2022)
19. E.Y. Nakanishi, M.R. Cabral, P. de Souza Gonçalves, V. dos Santos, H. Savastano Jr., *J. Clean Prod.* **195**, 1259 (2018)
20. I.R. Campbell, M.-Y. Lin, H. Iyer, M. Parker, J.L. Fredricks, K. Liao, A.M. Jimenez, P. Grandgeorge, E. Roumeli, *Annu. Rev. Mater. Res.* **53**, 81 (2023)
21. J.L. Fredricks, A.M. Jimenez, P. Grandgeorge, R. Meidl, E. Law, J. Fan, E. Roumeli, *J. Polym. Sci.* **61**(21), 2585 (2023)
22. H. Iyer, P. Grandgeorge, A.M. Jimenez, I.R. Campbell, M. Parker, M. Holden, M. Venkatesh, M. Nelsen, B. Nguyen, E. Roumeli, *Adv. Funct. Mater.* **33**, 2302067 (2023)
23. K. Liao, P. Grandgeorge, A.M. Jimenez, B.H. Nguyen, E. Roumeli, *Sustain. Mater. Technol.* **36**, e00591 (2023)
24. I.R. Campbell, Z. Dong, P. Grandgeorge, A.M. Jimenez, E.R. Rhodes, E. Lee, S. Edmundson, C.V. Subban, K.G. Spreng, E. Roumeli, “The role of biomolecular building blocks on the cohesion of biomatter plastics” (2024), Preprint. [https://papers.ssrn.com/sol3/papers.cfm?abstract\\_id=4734573](https://papers.ssrn.com/sol3/papers.cfm?abstract_id=4734573)
25. C. Simon, M. McHale, R. Sulpice, *Biology* (Basel) **11**(11), 1593 (2022)
26. A. Moreira, S. Cruz, R. Marques, P. Cartaxana, *Rev. Aquac.* **14**, 5 (2022)
27. H. Dominguez, E.P. Lorent, *Mar. Drugs* **17**, 357 (2019)
28. J.J. Bolton, M.D. Cyrus, M.J. Brand, M. Joubert, B.M. Macey, *Perspect. Phycol.* **3**(3), 113 (2016)
29. S. Gautam, A. Mogal, “Recent Advances in Composites from Seaweeds,” in *Composites from the Aquatic Environment*, ed. by S.S.M. I. Ahmad, Composites Science and Technology Book Series (Springer, Singapore, 2023), pp. 275–291
30. D.-H. Li, Z.-M. Han, Q. He, K.-P. Yang, W.-B. Sun, H.-C. Liu, Y.-X. Zhao, Z.-X. Liu, C.-N.-Y. Zong, H.-B. Yang, Q.-F. Guan, S.-H. Yu, *Adv. Mater.* **35**, 2208098 (2023)
31. B. Gwózdź, J.S. Schikan, “The Seaweed Archives: A Material Study of Seaweed as a Building Material and Its Implementation on Two Buildings on North Koster, Sweden,” Master’s thesis, Chalmers University of Technology (2022)
32. A. Israel, M. Shpigel, *J. Appl. Phycol.* **35**(5), 1987 (2023)
33. S. Revathi, R. Suganya, A. Haamidh, *Mater. Today* **64**, 814 (2022)
34. M. Nuopponen, T. Vuorinen, S. Jämsä, P. Viitaniemi, *Wood Sci. Technol.* **37**, 109 (2003)
35. G. Sinn, A. Reiterer, S.E. Stanzl-Tschegg, *J. Mater. Sci.* **36**, 4673 (2001)
36. D. Kocaeefe, X. Huang, Y. Kocaeefe, Y. Boluk, *Surf. Interface Anal.* **45**, 639 (2013)
37. G. Beamson, D. Briggs, *High Resolution XPS of Organic Polymers: The Scienta ESCA300 Database* (Wiley, Chichester, 1992)
38. P.G. Rouxhet, M.J. Genet, *Surf. Interface Anal.* **43**, 1453 (2011)
39. G. Greczynski, L. Hultman, *Vacuum* **205**, 111463 (2022)
40. G.N. Inari, M. Petrisans, J. Lambert, J.J. Ehrhardt, P. Gérardin, *Surf. Interface Anal.* **38**, 1336 (2006)
41. A. Pizzi, “Melamine-Formaldehyde Adhesives,” in *Handbook of Adhesive Technology*, vol. 2 (Marcel Dekker, New York, 2003), chap. 32
42. T.H. Jatmiko, D.J. Prasetyo, C.D. Poeloengasih, Hernawan, Y. Khasanah, “Nutritional Evaluation of *Ulva* sp. from Sepanjang Coast, Gunungkidul, Indonesia,” *IOP Conf. Ser. Earth Environ. Sci.* **251**(1), 012011 (2019)
43. J. Werkelin, B.-J. Skrifvars, M. Hupa, *Biomass Bioenergy* **29**, 451 (2005)



44. H. Vahabi, F. Laoutid, M. Mehrpouya, M.R. Saeb, P. Dubois, *Mater. Sci. Eng. R Rep.* **144**, 100604 (2021)
45. A.R. Angell, L. Mata, R. de Nys, N.A. Paul, *J. Appl. Phycol.* **28**, 511 (2016)
46. O. Benjama, P. Masniyom, *Songklanakarin J. Sci. Technol.* **33**(5), 575 (2011)
47. T.D. Schowalter, J.J. Morrell, *Wood Fiber Sci.* **34**(1), 158 (2002)
48. M. Dunky, *Int. J. Adhes. Adhes.* **18**, 95 (1998)
49. J. Chrobak, J. Iłowska, A. Chrobok, *Molecules* **27**, 4862 (2022)
50. D.A.L. Silva, N.C. Mendes, L.D. Varanda, A.R. Ometto, F.A.R. Lahr, "Life Cycle Assessment of Urea Formaldehyde Resin: Comparison by CML (2001), EDIP (1997) and USEtox (2008) Methods for Toxicological Impact Categories," in *Re-engineering Manufacturing for Sustainability, Proceedings of the 10th CIRP International Conference on Life Cycle Engineering*, ed. by A.Y.C. Nee, B. Son, S.-K. Ong (Singapore, April 17–19, 2013), pp. 529–534
51. A.M. Ferreira, J. Pereira, M. Almeida, J. Ferra, N. Paiva, J. Martins, F.D. Magalhães, L.H. Carvalho, *Polymers* (Basel) **10**, 1070 (2018)
52. Y. Yuan, M. Guo, *Int. J. Life Cycle Assess.* **22**, 1318 (2017)
53. A. Arias, S. González-García, S. González-Rodríguez, G. Feijoo, M.T. Moreira, *Sci. Total Environ.* **738**, 140357 (2020)
54. H.-K. Huang, C.-H. Hsu, P.-K. Hsu, Y.-M. Cho, T.-H. Chou, Y.-S. Cheng, *Biomass Convers. Biorefin.* **12**, 633 (2022)
55. J.X. Lim, T.K. Ong, C.K. Ng, I.W. Chua, Y.B. Lee, Z.Y. Yap, R.A. Bakar, *J. Phys. Conf. Ser.* **2120**, 012034 (2021)
56. A. Lakshmanan, B.S. Manjunatha, S. Bhowmick, A. Tewari, S. Nath Chattopadhyay, *Mater. Today* **76**, 239 (2023)
57. H. Baumann, A. Tillman, *Int. J. Life Cycle Assess.* **11**, 142 (2006)
58. D.J. Rose, L.G. Hemery, *J. Mar. Sci. Eng.* **11**(1), 175 (2023)
59. S. Wang, W. Wang, H. Yang, *Int. J. Environ. Res. Public Health* **15**, 2060 (2018)
60. M. Mironiuk, K. Chojnacka, "The Environmental Benefits Arising from the Use of Algae Biomass in Industry," in *Algae Biomass: Characteristics and Applications: Towards Algae-based Products*, ed. by K. Chojnacka, P.P. Wiecezorek, G. Schroeder, I. Michalak (Springer, Cham, 2018), pp. 7–16
61. Y. Zheng, R. Jin, X. Zhang, Q. Wang, J. Wu, *Stoch. Environ. Res. Risk Assess.* **33**, 1203 (2019)
62. M. Troell, P.J.G. Henriksson, A.H. Buschmann, T. Chopin, S. Quahe, *Rev. Fish. Sci. Aquac.* **31**(3), 285 (2023)
63. R. van Oirschot, J.-B.E. Thomas, F. Gröndahl, K.P.J. Fortuin, W. Brandenburg, J. Potting, *Algal Res.* **27**, 43 (2017)
64. D.A.L. Silva, A.S. Firmino, F.S. Ferro, A.L. Christoforo, F.R. Leite, F.A.R. Lahr, K. Kellens, *Int. J. Life Cycle Assess.* **25**, 1059 (2020)
65. P. Ngamnikom, S. Songsermpong, *J. Food Eng.* **104**, 632 (2011)
66. C.K. de Carvalho Araújo, M. Bigarelli Ferreira, R. Salvador, C.K.C. de Carvalho Araújo, B.S. Camargo, S.K. de Carvalho Araújo Camargo, C.I. de Campos, C.M. Piekarski, *J. Clean. Prod.* **355**(3), 131729 (2022)
67. S. Kakadellis, Z.M. Harris, *J. Clean. Prod.* **274**, 122831 (2020)
68. K. Sahoo, R. Bergman, S. Alanya-Rosenbaum, H. Gu, S. Liang, *Sustainability* **11**, 4722 (2019)
69. A. Besserer, S. Troilo, P. Girods, Y. Rogaume, N. Brosse, *Polymers* (Basel) **13**(11), 1752 (2021)
70. G. Gao, A.S. Clare, C. Rose, G.S. Caldwell, *Glob. Change Biol. Bioenergy* **10**, 39(2018)
71. S. Tsubaki, H. Nishimura, T. Imai, A. Onda, M. Hiraoka, *Sci. Rep.* **10**, 20399 (2020)
72. M. Koesling, N.P. Kvasdheim, J. Halfdanarson, J. Emblemsvåg, C. Rebours, *J. Clean. Prod.* **307**, 127301 (2021)
73. L. Hasselström, J.-B.E. Thomas, *Clean. Environ. Syst.* **6**, 100093 (2022)
74. L. Bushi, J. Meil, G. Finlayson, *A Cradle-to-Gate Life Cycle Assessment of North American Wood Product Resin Systems* (Athena Sustainable Materials Institute, Ottawa, 2022), pp. 1–93
75. O. Kelleci, S.E. Koksul, D. Aydemir, S. Sancar, *J. Clean. Prod.* **379**, 134785 (2022)
76. D. Krause-Jensen, C.M. Duarte, *Nat. Geosci.* **9**, 737 (2016)
77. C.M. Duarte, A. Delgado-Huertas, E. Marti, B. Gasser, I. San Martin, A. Cousteau, F. Neumeyer, M. Reilly-Cayten, J. Boyce, T. Kuwae, M. Hori, T. Miyajima, N.N. Price, S. Arnold, A.M. Ricart, S. Davis, N. Surugau, A.-J. Abdul, J. Wu, X. Xiao, I.K. Chung, C.G. Choi, C.F.A. Sondak, H. Albasri, D. Krause-Jensen, A. Bruhn, T. Boderskov, K. Hancke, J. Funderud, A.R. Borrero-Santiago, F. Pascal, P. Joanne, L. Ranivoarivelo, W.T. Collins, J. Clark, J.F. Gutierrez, R. Riquelme, M. Avila, P.I. Macreadie, P. Masque, Carbon burial in sediments below seaweed farms (2023), Preprint, bioRxiv. <https://doi.org/10.1101/2023.01.02.522332>
78. L. McClenachan, A. Moulton, *Mar. Policy* **146**, 105312 (2022)
79. N. Gopal, H.M. Hapke, K. Kusakabe, S. Rajaratnam, M.J. Williams, *Gen. Technol. Dev.* **24**(1), 1 (2020)
80. A.L.V. Espada, K.A. Kainer, *Land Use Policy* **127**, 106560 (2023)
81. M.S. Toivonen, S. Kurki-Suonio, F.H. Schacher, S. Hietala, O.J. Rojas, O. Ikkala, *Biomacromolecules* **16**, 1062 (2015)
82. M. Dunky, "Natural Crosslinkers for Naturally-Based Adhesives," in *Biobased Adhesives: Sources, Characteristics and Applications*, ed. by M. Dunky, K.L. Mittal (Wiley, New York, 2023), chap. 6, pp. 207–254
83. N. Fairley, V. Fernandez, M. Richard-Plouet, C. Guillot-Deudon, J. Walton, E. Smith, D. Flahaut, M. Greiner, M. Biesinger, S. Tougaard, D. Morgan, J. Baltrusaitis, *Appl. Surf. Sci. Adv.* **5**, 100112 (2021)
84. A.N. Myers-Pigg, S.C. Pennington, K.K. Homolka, A.M. Lewis, O. Otenburg, K.F. Patel, P. Regier, M. Bowe, M.I. Boyanov, N.A. Conroy, D.J. Day, C.G. Norris, E.J. O'Loughlin, J.A. Roebuck, L. Stetten, V.L. Bailey, K.M. Kemner, N.D. Ward, *Sci. Data* **10**, 822 (2023) □

#### Publisher's note

Springer Nature remains neutral with regard to jurisdictional claims in published maps and institutional affiliations.

Springer Nature or its licensor (e.g. a society or other partner) holds exclusive rights to this article under a publishing agreement with the author(s) or other rightsholder(s); author self-archiving of the accepted manuscript version of this article is solely governed by the terms of such publishing agreement and applicable law.